Effects of Structural, Electrical and Raman Properties of Al-Doped TiO_2 Thin Films Acquired by Sol-gel Spin Coating Method

Nor Damsyik Mohd Said[1]*, Mohd Zainizan Sahdan[2] and Feri Adriyanto[3]

[1]Department of Electrical Engineering,
Politeknik Mersing,
Jalan Nitar, 86800 Mersing, Johor, Malaysia.

[2]Faculty of Technical and Vocational Education,
Universiti Tun Hussein Onn Malaysia,
Persiaran Tun Dr. Ismail, 86400 Parit Raja, Johor, Malaysia.

[3]Department of Electrical Engineering,
Sebelas Maret University,
Jl. Ir. Sutami No 36A-Kentingan Surakarta, 57126 Indonesia.

*Corresponding Author's Email: nordamsyik@gmail.com

Article History: Received 19 July 2024; Revised 27 November 2024; Accepted 27 November 2024

Abstract

Titanium dioxide (TiO2) is well known for its excellent photocatalytic properties and potential applications, particularly in gas sensing. However, its high resistivity can limit its performance in such applications. This study explores the effect of aluminium (Al) doping on the structural, electrical, and Raman properties of TiO2 thin films, to optimise their performance for gas sensor applications. TiO2 films were prepared with varying Al concentrations (1 wt.%, 2 wt.%, 3 wt.%, 4 wt.%, 5 wt.%, and 6 wt.%) using the sol-gel spin coating method. The films were characterised using X-ray diffraction (XRD), current-voltage (IV) measurements, and Raman spectroscopy. The results show that doping with 3 wt.% Al significantly improves the structural, electrical, and Raman properties of the films, yielding the lowest resistivity value of 734.873 Ω-cm and the most pronounced anatase peak in the Raman spectra. These findings indicate that 3 wt.% Al doping optimises TiO2 thin films for gas sensor applications, offering potential improvements for environmental and industrial sensing technologies.

Keywords: Al Doping Concentration, Inorganic Semiconductor, Nanomaterials, Sol-gel, Spin Coating

1.0 Introduction

Titanium dioxide (TiO_2) has garnered significant attention in recent years due to its exceptional chemical and mechanical stability, non-toxicity, low cost [1], and flexibility, making it a promising material for various modern technologies, including solar cells [2] and gas sensors [3]. Despite its advantages, TiO_2 suffers from high charge carrier recombination rates, which limits its efficiency in applications. One effective way to address this issue is by doping TiO_2 with aluminium (Al), which has been shown to reduce resistivity and enhance charge carrier concentration [4]. This study explores the effect of varying Al concentrations (1 wt.%, 2 wt.%, 3 wt.%, 4 wt.%, 5 wt.%, and 6 wt.%) on the structural, electrical, and Raman properties of TiO_2 thin films, aiming to optimise their performance for gas sensor applications. TiO_2 films were prepared using the sol-gel spin coating method and characterised via X-ray diffraction (XRD), current-voltage (IV) measurements, and Raman spectroscopy. Results indicate that 3 wt.% Al doping significantly improves the structural, electrical, and Raman properties, achieving the lowest resistivity value of 734.873 Ω-cm and the most pronounced anatase peak. These findings suggest that 3 wt.% Al-doped TiO_2 films could offer enhanced performance for gas sensor and solar cell applications, addressing the challenges associated with charge carrier recombination and paving the way for improved environmental and industrial sensing technologies.

Doping has emerged as a vital method for tailoring the electrical and chemical properties of TiO_2, enabling its use in various technological applications. By introducing impurities, the conductivity of TiO_2 can be modified from n-type to p-type, providing a versatile platform for applications in semiconductors, photocatalysts, and sensors. For example, impurities like aluminium (Al) and nitrogen (N) have been successfully doped into TiO_2 to enhance its photocatalytic and electrical properties [2], [3]. However, despite these advancements, the full potential of doping in TiO_2 remains underexplored, leaving room for further investigation.

Traditional methods of doping, such as diffusion and ion implantation, have been extensively studied and applied to TiO_2. Diffusion doping involves the movement of dopant atoms from a region of higher concentration to one of lower concentration, driven by random motion, while ion implantation entails bombarding the TiO_2 surface with high-energy ions [4]. Although these methods are effective, they often lead to inconsistencies in doping efficiency due to structural defects and phase transformations induced during the process. These inconsistencies highlight the need for innovative doping techniques to achieve uniform and stable results.

The choice of doping elements significantly impacts the resultant properties of TiO_2. Studies have shown that different dopants, such as Al, N, and Fe, alter phase relations, crystal size, resistivity values, and Raman peak shifts differently [5]. For instance, Al-doped TiO_2 thin films have exhibited enhanced conductivity but also introduced complex Raman shifts, which complicates the characterisation of their structural properties [6]. The challenge lies in selecting dopants that maximise desirable properties while minimising structural disruptions.

One of the major challenges in doping TiO_2 is managing the structural defects that arise during the process. Defects, such as oxygen vacancies and interstitials, can either enhance or hinder the desired properties depending on their concentration and interaction with dopant atoms [7]. While some defects are beneficial for enhancing conductivity, excessive defect formation can degrade the material's stability and performance. Understanding this delicate balance is essential for advancing doping techniques.

Although doping has demonstrated potential for improving TiO_2's electrical and photocatalytic performance, its long-term stability under environmental stress remains a critical issue. Factors such as thermal fluctuations, humidity, and prolonged exposure to ultraviolet light can alter the structural and electronic properties of doped TiO_2, leading to performance degradation over time [8], [9]. Addressing these concerns requires further investigation into the durability of doped TiO2 under real-world conditions.

To overcome the limitations of traditional methods, researchers have explored novel doping techniques, such as co-doping and plasma-assisted doping. Co-doping, which involves introducing multiple dopants simultaneously, has been shown to improve the synergistic effects of dopants, leading to enhanced properties [3]. Plasma-assisted doping, on the other hand, offers better control over dopant distribution and minimises structural damage, making it a promising alternative [10]. However, these techniques are still in their infancy and require further optimization for scalability.

Despite considerable progress, several research gaps remain in the field of TiO_2 doping. A deeper understanding of the interactions between dopants, defects, and the TiO_2 matrix is needed to optimise doping efficiency and reproducibility [11]. Additionally, the lack of comprehensive studies on the environmental and operational stability of doped TiO2 limits its practical applications. Therefore, the main purpose of this study is to explore the effect of aluminium (Al) doping on the structural, electrical, and Raman properties of TiO_2 thin films, to optimise their performance for gas sensor applications. By comprehensively exploring these effects, the study contributes to paving the way for more efficient and reliable use of doped TiO2 in advanced technologies [6].

2.0 Methodology

The materials used were titanium (IV) butoxide ($Ti(OC_4H_9)_4$ as precursor, ethanol as solvent (C_2H_5OH), deionized water as a function of adding the oxygen (O), acids and triton X-100 ($C_{14}H_{22}O(C_2H_4O)_n$) as a stabilizer to avoid precipitation in solution In addition, the type of acids were glacial acetic acid (CH_3CO_2H) and hydrochloric acid (HCl) also added to solution. For solution preparation, titanium (IV) butoxide mixed with ethanol, acid catalysts, triton X-100 and aluminium nitrate nanohydrate [$Al(NO_3)_3 \cdot 9H2O$; Sigma-Aldrich, ≥ 98%] were stirred for 3 hours for the ageing process at room temperature. The Al doping concentrations were 0wt.%, 1wt.%, 2wt.%, 3wt.%, 4wt.%, 5wt.%, and 6wt.%.

The acquired solution is spin-coated on a glass substrate at a speed of 3000 rpm for 30 s to form 5 layers of uniform films. TiO_2 solution was dropped up to 10 times onto the substrates. After spin–coating, the formed layer was preheated at 100 °C for 5 min. All layers were then annealed at 500 °C for one hour to achieve crystallisation. The structural properties were characterised by PAnalytical Smartpowder X-ray diffractometer (XRD). XRD is used to identify the crystallinity and phases of the Al-TiO_2 thin film. The measurement was obtained at 2θ degree by Cu Kα radiation. The electrical properties of the thin film were determined by doing the current-voltage (I-V) analysis on the thin film. Raman spectroscopy is to identify the Raman peak. The estimation of the crystal size, D according to Scherrer's equation (1):

$$D = \frac{0.9\lambda}{\beta \cos\theta} \quad (1)$$

where λ is the light wavelength, β is the full-width half maximum and θ is the degree of diffraction.

3.0 Results and Discussion

3.1 XRD Analysis

Figure 1 shows the XRD patterns of different Al doping concentrations (0 wt.%, 1 wt.%, 2 wt.%, 3 wt.%, 4 wt.%, 5 wt.% and 6 wt.%). It can be seen from the figure that the peak heights 233.8 cts, 108.8 cts, 101.5 cts, 103.7 cts and 77.28 cts correspond to 0 wt.%, 1 wt.%, 2 wt.%, 3 wt.% and 4 wt.% Al doping concentrations, respectively. All obtained thin films had an anatase peak and peak height lower than the pure TiO_2 (233.8 cts) due to an increase Al doping concentration.

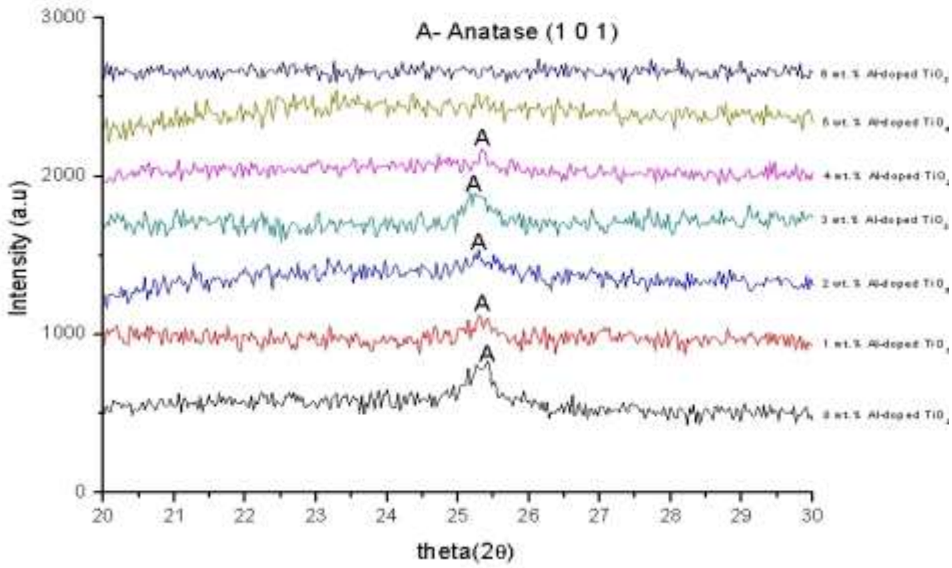

Figure 1: XRD patterns of different Al doping concentrations (0 wt.%, 1 wt.%, 2 wt.%, 3 wt.%, 4wt.%, 5wt.% and 6wt.%)

Generally, anatase has a small band gap. Such a small band gap reduces the light that can be observed and it might enhance the valence band into a higher energy level [5]. At 5 wt.% and 6 wt.% Al doping concentrations, there was no anatase peak. Anatase TiO_2 peaks developed minor with the rise of the Al doping concentration due to the disorder produced by the size of the ionic radii of Al^{3+} and Ti^{4+} [6]. Doping of Al into TiO_2 can indicate a crystallite-sized anatase TiO_2. Consequently, the crystallite sizes would be smaller paralleled to the pure thin films. According to Hanini et al., however, XRD showed almost the same peak compared the reported research (100 cts) [7]. This phenomenon was observed due to the reduced anatase peak in the increase of Al doping concentration [8]. This phase was thermodynamically stable due to being assigned with 101 facets and possessing the lowest surface area [6].

The difference Al doping concentration had a smaller crystal size 22.62 nm, 13.87 nm,18.85 nm and 10.39 nm corresponds to the 1 wt.%, 2 wt.%, 3 wt.% and 4 wt.% Al doping concentration, respectively, against the pure TiO_2 (22.62 nm) [9] when compared to the reported research that the crystal size was almost the same (11 nm to 26.2 nm) [6,123].

Table 1: Peak properties of Al-doped TiO_2 thin film with different Al doping concentrations (0 wt.%, 1 wt.%, 2 wt.%, 3 wt.%, 4wt.%, 5wt.% and 6wt.%)

Al-doped TiO_2 Con.	Position 2 thetas (°)	Intensity (cts)	FWHM, deg	Calculated crystallite size, D (nm)	Dislocation ($x10^{15}$)	Strain (%)	Stress GPa	Lattice constant (nm)	
								A	C
0 wt.%	25.3735	233.83	0.360	22.62	1.954	0.147	0.340	0.37760	0.94860
1 wt.%	25.3574	108.8	0.3542	22.62	1.892	0.105	-0.245	0.37800	0.95100
2 wt.%	25.3044	101.5	0.576	13.87	5.192	0.053	0.123	0.37860	0.94950
3 wt.%	25.2528	103.70	0.432	18.85	2.814	0.589	1.370	0.37960	0.94440
4 wt.%	25.3310	77.28	0.768	10.39	9.256	4.316	10.476	0.38070	0.90900

Table 1 reveals the peak properties of Al-doped TiO_2 thin film with different Al doping concentrations. The dislocations were $1.954x10^{15}$, $1.892x10^{15}$, $5.192 x10^{15}$, $2.814 x10^{15} nm^{-2}$ and $9.256 x10^{15}$ correspond to 0 wt.%, 1 wt.%, 2 wt.%, 3 wt.% and 4 wt.% Al doping concentrations, respectively. The decrease of dislocation indicated a decrease in defect concentration in the crystal lattice with an increase in Al doping concentration. According to Zhu et al., the value of the FWHM was less than with the reported research (0.45 to 0.78) due to the dislocations that were inhomogeneous and it produced the macro heterogeneity of the crystals [13]. This phenomenon was also observed by Raman [6].

The strains were 0.147%, 0.105%, 0.053%, 0.589% and 4.316% corresponding to 0 wt.%, 1 wt.%, 2 wt.%, 3 wt.% and 4 wt.% Al doping concentrations, respectively. When a 3 wt.% Al doping concentration was affected, the strain of the thin film added due to the strain energy that could limit the dopant solubility in the thin film [6]. According to Bensouici et al., the value of the strain was slightly higher compared to the reported research ($0.23x10^{-6}$) due to strain broadening from dislocations which affected the width of the diffraction peaks [14].

The stresses were 0.340, -0.245, 0.123, 1.370 and 10.476 GPa corresponding to 0 wt.%, 1 wt.%, 2 wt.%, 3 wt.% and 4 wt.% Al doping concentrations, respectively. All the thin films were tensile stress except 1 wt.% Al-doped TiO_2 due to the AFM results whereas the roughness is the highest compared with other thin films. When 3 wt.% Al doping concentration was affected, and the stress of the thin film produced a tensile thin film due to the positive sign due to the uniform distribution of the Al dopant [14]. At 3 wt.%, the value of the stress was the same as the reported research due to the stretching that occurred when a stretching force was applied to the thin film [14]. According to Pfeiffer et al., the value of the stress was slightly lower compared to the reported research (4 GPa) due to stress broadening from dislocations which affected the width of the diffraction peaks [16]. Then, the types of thin film were determined as either tensile or compressive thin film. If tensile, the thin film would be positively signed and if compressive, the thin film was negatively signed. In this case, the 3wt.% Al-doped TiO_2 thin film was a tensile thin film due to bending in the surface and it was adjusted to have concave geometry. It was also substitutional doping [17].

The insert to the Ti^{4+} ion was referred to as substitutional doping and the Al dopant dissolved well into the TiO_2 crystal [7]. At 3 wt.% Al doping concentrations, the value of lattice “a” increased and lattice “c” decreased compared to the reported research. Lattice “a” and “c” decreased due to the decreasing of the lattice constant “c” which indicated the Al^{3+} replaced Ti^{4+} in the lattice and formed a solid solution. Doping Al atoms added the lattice constant “a” of the tetragonal TiO_2 structure which can reveal that Al had inserted into the TiO_2 lattice.

XRD data states that Al ions dissolve in the TiO_2 lattice due to the similar ionic radius to Ti. At 3 wt.% Al doping concentration, the structural modification of the thin film was optimised due to the distorted anatase structure [18].

3.2 I-V Measurement

The electrical properties of the TiO_2 thin film for different Al doping concentrations were analysed using an IV-probe. Figure 2 shows the sheet resistance and resistivity measurement for difference Al doping concentrations.

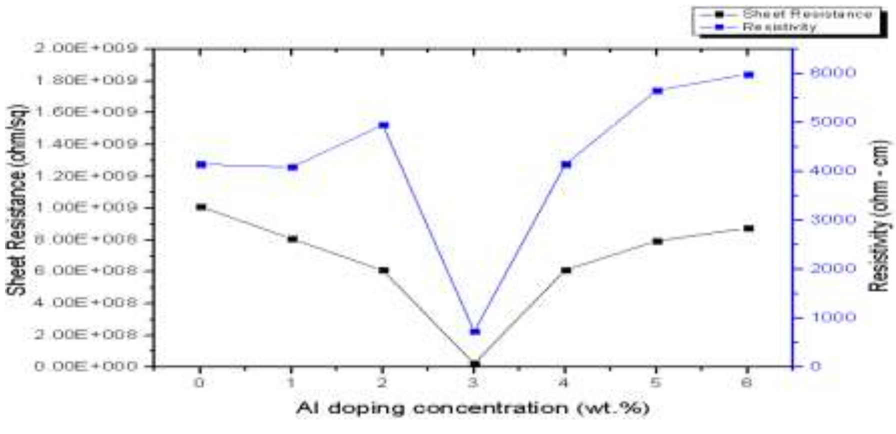

Figure 2: Sheet resistance and resistivity measurement for different Al doping concentrations (0 wt.%, 1 wt.%, 2 wt.%, 3 wt.%, 4wt.%, 5wt.% and 6wt.%)

The resistance and the resistivity of the Al-doped with TiO_2 depended on two factors, namely (i) the presence of a charge carrier doping concentration in the thin film and (ii) the mobility of the metal atom charge carriers [18]. The sheet resistance was proportional to the resistivity of the Al-doped TiO_2 thin film [20]. The sheet resistances were 1.01x10^9 Ω/sq, 8.07887x10^8 Ω/sq, 6.09x10^8 Ω/sq, 2.37056x10^7 Ω/sq, 6.10x10^8Ω/sq, 7.94x10^8Ω/sq and 8.75258x10^8Ω/sq corresponding to 0 wt.%, 1 wt.%, 2 wt.%, 3 wt.%, 4 wt.%, 5 wt.% and 6 wt.% Al- doped TiO_2, respectively. The pure TiO_2 thin film had a resistivity of 4150 Ω-cm. At 3 wt.% Al-doped TiO_2, the resistivity value achieved a minimum level of 734.873 Ω-cm lower resistivity compared to resistivity 4089.93 Ω-cm,49500 Ω-cm, 4147.3 Ω-cm, 5659.86 Ω-cm and 5990.90 Ω-cm at the extreme.

Thus, the mobility of the Al atom's charge carriers prevented the counteraction of this rise in the charge carrier concentration The valence electron of each Al atom was then free to move through the whole crystal structure and was no longer bound to the outer shell of any Al atom [21]. From the decrease in sheet resistance and resistivity, it was noted that the mobility of the Al atom charge carriers at the optimised doping concentration was significant enough to determine the decreasing resistivity of the thin film. The surface interaction between particles increased due to the increase in particle size which produced better electron mobility in the thin films. Therefore, the resistivity of the film decreased. The reported research found that the resistivity value of the Al-doped TiO_2 was around 1.05x10^5 Ω-cm [22]. It was perceived that the resistivity of the Al-doped TiO_2 for this research was much lower than the reported research [20]. The reported research found that the hall mobility was around 0.312(cm^2 / Vs) and carrier concentration 4.245×$10^{15}cm^{-3}$ [22]. The sheet resistance (2.37056x10^7 Ω/sq), and the resistivity (734.873 Ω-cm) were lower than other thin films as shown in Figure 4.15. The lower sheet resistance and the mobility of the charge carriers were greater than the rise in the concentration of the charge carriers. After that, the process of optimisation was determined [24].

3.3 Raman Analysis

Therefore, the Raman spectrum of the pure TiO_2 and Al-doped TiO_2 thin films was recorded at room temperature at a spectral range of 50 to 800 cm^{-1} as shown in Figure 3. The intensity peak at 144.913 cm^{-1} increased with increasing doping temperature. Therefore, it might be believed that an increase in peak intensity was due to a high crystallinity film. When the thin film was characterised using Raman Spectroscopy, the thin films were determined to have an anatase peak. In this case, the anatase peak was (34912.39 a.u) at 3 wt.% Al doping which was higher than the pure TiO_2 (9776.157 a.u), 1 wt.% (8930.329 a.u), 2wt.% (9753.12 a.u) and 4wt.% (19028.8 a.u) because of the raise in the Al doping concentration. At 5 wt,% and 6wt.% there no anatase peak due to the increase in the Al doping concentration. The shrillest and strongest peak at 147 cm^{-1} was allocated to the high-frequency branch of the E_g mode of 3 wt.% Al-doped TiO_2, which was the strongest mode in the anatase phase. The anatase peak was allocated to the high frequency of the E_g mode of the 3 wt.% Al-doped TiO_2 branch. This showed the good crystallinity [19]. Furthermore, FWHM showed Al-doped TiO_2 at the strongest peak, significance that the FWHM reduced when the doping concentration was raised. The Raman spectra were consistent with the results revealed from the XRD analysis [19].

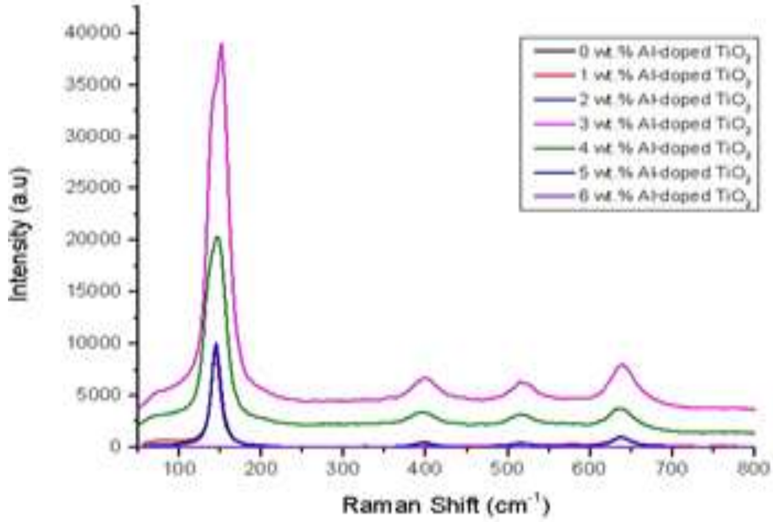

Figure 3: Raman Spectra of different Al doping concentrations (0 wt.%, 1 wt.%, 2 wt.%, 3 wt.%, 4wt.%, 5wt.% and 6wt.%)

The Raman spectrum of 3 wt.% Al-doped TiO_2 showed broadening in each mode of vibration and shifting in the E_g mode as compared to the pure TiO_2. This could be ascribed to a decrease in particle size affecting the phonon modes and the electron-phonon interaction. The intensity of the anatase peak of 3 wt.% Al-doped TiO_2 was approximate to the reported research (34912.39 a.u) [18].

4.0 Conclusion

In conclusion, the objective of this study was successfully achieved by exploring the effect of aluminium (Al) doping on the structural, electrical, and Raman properties of TiO2 thin films, with the aim of optimising their performance for gas sensor applications. Aluminium-doped TiO2 thin films were prepared using the sol-gel spin coating technique, and their structural characteristics were found to be similar to those of undoped TiO2, exhibiting anatase nanocrystalline structures. The study optimised the doping concentration at 3 wt.% Al, which significantly influenced the electrical and Raman properties of the films. The electrical resistivity of the 3 wt.% Al-doped TiO2 thin film was notably reduced to 734.873 Ω-cm, with higher aluminium content leading to a more pronounced anatase Raman peak. These results demonstrate that the 3 wt.% Al-doped TiO2 thin film offers the best performance in terms of structural, electrical, and Raman properties, making it a promising candidate for gas sensor applications. The findings highlight the potential of aluminium doping as an effective method to enhance the performance of TiO2-based materials for advanced technological applications.

Acknowledgement

The authors would like to acknowledge the Ministry of Education Malaysia for the funding via FRGS grant vote 1507 and Universiti Tun Hussein Onn Malaysia (UTHM) for the technological services. The authors also wish to thank Jabatan Pendidikan Politeknik dan Kolej Komuniti (JPPKK), and Politeknik Mersing for support and technical guidance.

Author Contributions

N. D. Mohd Said: Conceptualization, Methodology, Software, Writing-Original Draft Preparation; **M. Z. Sahdan:** Data Curation, Validation, Supervision; **F. Adriyanto:** Validation, Writing-Reviewing and Editing.

Conflicts of Interest

The manuscript has not been published elsewhere and is not under consideration by other journals. All authors have approved the review, agree with its submission, and declare no conflict of interest in the manuscript.

References

[1] A. Schaefer, V. Lanzilotto, U. Cappel, P. Uvdal, A. Borg, and A. Sandell, “First layer water phases on anatase TiO2(101),” *Surface Science*, vol. 674, pp. 25–31, 2018.

[2] A. Ranjitha, M. Thambidurai, F. Shini, N. Muthukumarasamy, and D. Velauthapillai, “Effect of doped TiO2 film as electron transport layer for inverted organic solar cell,” *Materials Science for Energy Technologies*, vol. 2, no. 3, pp. 385–388, 2019.

[3] K. D. Benkstein and S. Semancik, “Mesoporous nanoparticle TiO2 thin films for conductometric gas sensing on microhotplate platforms,” *Sensors and Actuators B: Chemical*, vol. 113, no. 2, pp. 445–453, 2006.

[4] W. Zhang, X. Pei, J. Chen, and H. He, “Effects of Al doping on properties of xAl–3%In–TiO2 photocatalyst prepared by a sol–gel method,” *Materials Science in Semiconductor Processing*, vol. 38, pp. 24–30, Oct. 2015.

[5] X. Xue et al., “Effects of Mn doping on surface enhanced Raman scattering properties of TiO2 nanoparticles,” *Spectrochimica Acta Part A: Molecular and Biomolecular Spectroscopy*, vol. 95, pp. 213–217, 2012.

[6] D. M. De Los Santos, J. Navas, A. Sánchez-Coronilla, R. Alcántara, C. Fernández-Lorenzo, and J. Martín-Calleja, “Highly Al-doped TiO2 nanoparticles produced by ball mill method: Structural and electronic characterization,” *Materials Research Bulletin*, vol. 70, pp. 704–711, 2015.

[7] F. Hanini et al., “Characteristics of Al-doped TiO2 thin films grown by pulsed laser deposition,” *International Journal of Nanoparticles*, vol. 6, no. 2–3, 2013.

[8] N. D. Mohd Said et al., “Difference in structural and chemical properties of sol-gel spin-coated Al-doped TiO2, Y-doped TiO2 and Gd-doped TiO2 based on trivalent dopants,” *RSC Advances*, vol. 8, no. 52, pp. 29686–

29697, 2018.

[9] N. D. Said, "A study of TiO2 thin film using sol-gel method," *Politeknik & Kolej Komuniti Journal of Engineering and Technology*, vol. 1, no. 1, pp. 77–84, Nov. 2016.

[10] K. Sahu and V. V. S. Murty, "Novel sol-gel method of synthesis of pure and aluminium doped TiO2 nanoparticles useful for dye-sensitized solar cell applications," *Indian Journal of Pure and Applied Physics*, vol. 54, no. 8, pp. 485–488, 2016.

[11] Y. J. Choi, Z. Seeley, A. Bandyopadhyay, S. Bose, and S. A. Akbar, "Aluminum-doped TiO2 nano-powders for gas sensors," *Sensors and Actuators B: Chemical*, vol. 124, no. 1, pp. 111–117, 2007.

[12] K. Sahu and V. V. S. Murty, "Novel sol-gel method of synthesis of pure and aluminum doped TiO2 nanoparticles," *Indian Journal of Pure and Applied Physics*, vol. 54, no. 8, pp. 485–488, 2016.

[13] J. Zhu, W. Zhang, W. Yan, H. Yang, L. Huang, and H. Li, "Al-doped TiO2 mesoporous material supported Pd with enhanced catalytic activity for complete oxidation of ethanol," *Journal of Solid State Chemistry, vol. 248,* pp. 142–149, 2017.

[14] F. Bensouici, M. Bououdina, M. Trari, and R. Belkada, "Al doping effect on the morphological, structural and photocatalytic properties of TiO2 thin layers," *Thin Solid Films*, vol. 616, pp. 655–661, 2016.

[15] C. Zhang, Y. Qi, S. Liu, Y. Men, and F. Cui, "Novel mesoporous Al-doped TiO2 with improved lithium storage performance," *Materials Chemistry and Physics*, vol. 237, p. 121822, 2019.

[16] S. Pfeiffer, K. Scharvogel, G. Gruner, and A. Greil, "Crack-reduced alumina/aluminum titanate composites additive manufactured by laser powder bed fusion of black TiO2−x doped alumina granules," *Journal of the European Ceramic Society*, vol. 42, no. 8, pp. 3515–3529, 2022.

[17] P. M. Kibasomba, K. H. Mutombo, A. Manyala, P. M. Kamga, and J. M. Kiat, "Strain and grain size of TiO2 nanoparticles from TEM, Raman spectroscopy and XRD: The revisiting of the Williamson-Hall plot method," *Results in Physics*, vol. 9, pp. 628–635, 2018.

[18] J. García, A. Neftalí, C. Mendoza, P. Marcela, and M. Romero, "Improvement of the morphological and electrical characteristics of Al3+, Fe3+, and Bi3+-doped TiO2 compact thin films and their incorporation into hybrid solar cells," *Materials Science in Semiconductor Processing*, vol. 72, pp. 106–114, 2017.

[19] F. Bayata and M. Ürgen, "Role of aluminum doping on phase transformations in nanoporous titania anodic oxides," *Journal of Alloys and Compounds*, vol. 646, pp. 719–726, Oct. 2015.

[20] R. Valaski, C. Arantes, C. A. Senna, V. Carôzo, C. A. Achete, and M. Cremona, "Enhancement of open-circuit voltage on organic photovoltaic devices by Al-doped TiO2 modifying layer produced by sol-gel method," *Thin Solid Films*, vol. 572, pp. 2–7, 2014.

[21] S.-S. Lin and D.-K. Wu, "Enhanced optical properties of Al-doped TiO2 thin films in oxygen or nitrogen atmosphere," *Applied Surface Science*,

vol. 255, no. 20, pp. 8654–8659, Jul. 2009.

[22] M. Z. Musa, K. A. Kasbi, A. A. Aziz, M. S. P. Sarah, M. H. Mamat, and M. Rusop, "Aluminium doping of titanium dioxide thin films using sol–gel method," *Materials Research Innovations*, vol. 15, no. s2, pp. s137–s140, Aug. 2011.

[23] S. Bhat, K. M. Sandeep, P. Kumar, M. P. Venu, S. M. Dharmaprakash, and J. S. Bhat, "Effect of Al doping on the carrier transport characteristics of TiO2 thin films anchored on glass substrates," *Applied Physics A: Materials Science and Processing*, vol. 125, no. 3, pp. 1–11, 2019.

[24] Y. C. Chung, P. J. Cheng, Y. H. Chou, B. T. Chou, K. B. Hong, J. H. Shih, S. D. Lin, T. C. Lu, and T. R. Lin, "Surface roughness effects on aluminium-based ultraviolet plasmonic nanolasers," *Scientific Reports*, vol. 7, no. 1, p. 39813, Jan. 2017.